Journal of Medical Systems (2019) 43: 22
https://doi.org/10.1007/s10916-018-1142-z

IMAGE & SIGNAL PROCESSING

Study on Brain Electromyography Rehabilitation System Based on Data Fusion and Virtual Rehabilitation Simulation

Shuxia Li [1] · Juncheng Yang [1]

Received: 26 November 2018 / Accepted: 17 December 2018 / Published online: 2 January 2019

Abstract

In this paper, a virtual rehabilitation training system based on electroencephalogram (EMG) feedback is proposed to solve the problem that the existing virtual rehabilitation training methods can not reflect the initiative of patients and lack of individual adaptability. Aiming at the EEG data fusion rehabilitation system based on Virtual Prototyping technology, a motion pattern recognition method based on the feature fusion of EEG and EMG signals is studied to improve the accuracy and flexibility of the rehabilitation training system. The corresponding virtual rehabilitation training scene is designed, and the control and feedback adjustment of the virtual scene are realized by using the above EEG feature analysis method. Finally, the virtual rehabilitation training is realized. The multi-level coupling relationship between EEG and EMG signals under different grip forces was explored by using the synchronous coupling characteristics between EEG and EMG signals, which provided a theoretical basis for further application in clinical rehabilitation evaluation.

Keywords Virtual prototyping technology · EEG data · EMG data · Rehabilitation system · Data fusion

Introduction

In recent years, with the rapid development of computer technology, research institutions at home and abroad have introduced virtual reality technology into the field of rehabilitation and Research on new rehabilitation methods. For example, Choi C and others have developed a computer interface based on surface electromyography signal and virtual reality, and applied to spinal cord injury patients [1]. These rehabilitation methods can enhance the interest and confidence of patients in training through virtual scenes, and have a certain degree of interest and flexibility, but there are still shortcomings in the individual adaptability of patients, active participation, operational safety and feasibility [2]. If the system is difficult to adjust and control the patient's subjective intention and rehabilitation status, patients are prone to spasm, muscle strain and other accidents during long-term, high-speed or large-scale training, resulting in secondary injury. Bioelectrical signals and EMG signals directly reflect the intention of human movement, but also often contain a large number of information reflecting the functional status of the patients'motor nervous system [3, 4]. Therefore, the rehabilitation training system based on biofeedback has gradually become a research hotspot. For example, brain-computer interface technology is used to achieve virtual reality rehabilitation training, and better training results are obtained; by extracting the arm surface electromyogram signal and motion sensor signal, rehabilitation training is completed with the help of virtual reality technology.

However, because patients are susceptible to fatigue during rehabilitation exercise, a series of changes have taken place in EEG and EMG signals, which will affect the rehabilitation effect. Appropriate training considering the fatigue state of patients can help patients improve their confidence in rehabilitation, enhance their active participation, and then make rehabilitation training more intelligent and humanized, while improper training intensity brings the possibility of secondary injury to patients [5]. Therefore, it is necessary to adjust the control parameters of the virtual scene in real time and the training content adaptively based on the fatigue state of the patients. At the same time, on the one hand, EEG has the characteristics of weakness, aliasing and low signal-to-noise

This article is part of the Topical Collection on *Image & Signal Processing*

✉ Juncheng Yang
juncheng@126.com

1 School of Electronic and Information Engineering, Henan Polytechnic Institute, Zhengzhou, China

ratio [6, 7]. On the other hand, the inadequate motor function and long-term exercise of patients are prone to fatigue, muscle weakness and other conditions, which make the fatigue estimation accuracy based on EEG fatigue characteristics or sEMG fatigue characteristics reduced, affecting the training effect [8] Therefore, it is necessary to extract EEG and sEMG signals synchronously, comprehensively consider the characteristics of brain fatigue and muscle fatigue, and adjust the training content in real time based on the fatigue state of patients, so as to obtain better rehabilitation effect.

Virtual prototyping technology

Technical introduction

The virtual prototyping technology used in this project is a digital design technology based on virtual prototyping, mainly used in the field of design and manufacturing. This project uses MSC Adams software to complete the design.

This series of software is developed by American scientists. Subsequently, the simulation software that appeared in the development of the American MSC company is also the mainstream mechanical dynamic simulation software of today. The software is widely used in engineering equipment, road and bridge structure, aerospace, industrial machinery and vehicle engineering. Its software module consists of five basic modules: basic module, extension module, interface module, professional domain module and toolbox module [9]. According to the design goal, the virtual prototype model of multi-body dynamics, which integrates mechanical, electrical, hydraulic and multi-system, is generated by the software. Through the analysis and demonstration of the combined correlation model, the product quality can be improved through modification, and the research and development cycle from design to finished product can be greatly shortened.

Virtual prototyping technology is being widely used in different applications. For the concept of virtual prototyping, the following is a description of the US Department of Defense [9]:

(1) Virtual prototyping technology is to build a prototype system or subsystem model on a computer.
(2) The virtual prototype can simulate the design model or the characteristics of the subsystem using the virtual prototype, which can replace the traditional physical prototype to a certain extent.
(3) For the virtual prototype design environment, its essence is a collection consisting of simulation, simulator and model.

Virtual prototyping technology has lower cost and faster speed. The lower cost saves the system a high cost of building a physical prototype in the past. While saving cost, virtual prototyping technology is far less than physical prototyping technology in the establishment of system cycle. Virtual prototyping technology has great advantages in optimizing design. Because of its convenience for modification, virtual prototyping technology is often used to analyze and compare various design schemes and select the best one. Virtual prototyping technology supports a variety of design methods, so that it can achieve multi-expert collaborative design and upstream and downstream concurrent design through concurrent design.

Establishment process of virtual prototyping system

Virtual prototyping technology refers to the process of product design and development, the scattered parts of the design and analysis technology together, in the computer to build the overall model of the product [10]. A new technology is proposed to predict the overall performance of the product, improve the design and improve the performance of the product. The flow chart of virtual prototyping modeling is shown in Fig. 1. CAD modeling is the basis of virtual prototyping modeling, mainly through computer-aided design.

(1) Model creation

Common models can be extracted and used directly from the Adams / View parts library; however, for complex or unusual models, it is necessary to import them through other CAD software. Because the robot is a special model, it must be imported from other software.

(2) Model test

The software design is more humanized, so that the application personnel can carry out kinematics simulation and

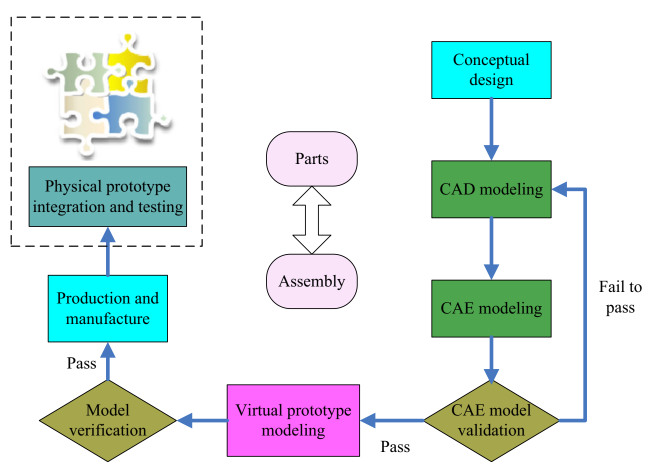

Fig. 1 Flow chart of virtual prototype modelling

verify the design model when the model is finished or even in the process. In the process of motion simulation, software can analyze motion characteristics, such as speed and displacement data. In the simulation process, the result is displayed intuitively by the measuring line.

(3) Model verification

The physical test data is imported and displayed in the superposition curve. By comparing and analyzing the results, it is convenient for designers to verify and make timely modifications.

(4) Model optimization

After determining the basic motion of the model, complex parameters (increasing rigid deformation, increasing the constraint between objects, modifying the friction coefficient, etc.) can be added to the model, and the model design can be gradually improved according to the simulation results [11]. Design points and design variables can also be defined to facilitate the comparison of different design schemes, so that we can modify the parameters of the model and optimize the design.

Acquisition and pretreatment of EEG signals

EEG signal acquisition

The acquisition system of EEG signals consists of two parts, including hardware and software. The hardware part includes EMG collector, EMG electrode, EEG cap, EEG collector and data acquisition card. The software mainly includes storing, analyzing and displaying the EEG signals and virtual scene. The block diagram of the whole EEG signal acquisition system is shown in Fig. 2.

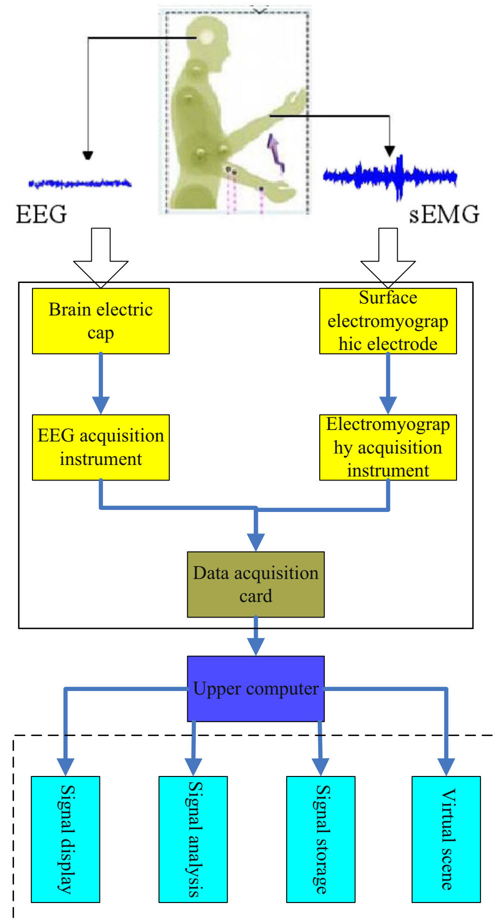

Fig. 2 Block diagram of EEG signal acquisition system

EEG signal preprocessing

Since EMG signals are mainly affected by power frequency, motion interference and harmonics, EEG signals are mainly affected by EMG, Eye and power frequency interference [12]. In this chapter, adaptive high-pass filter is used to remove the baseline drift in EEG signals. Adaptive filter is designed based on adaptive notch filter and an adaptive notch filter is used to remove 50 Hz power frequency interference in EEG signals.

Low pass filtering

The main function of digital filters is to filter the discrete time series with fixed frequency band. The common types of digital filters include finite impulse response digital filters and infinite impulse response digital filters. IIR filter is mainly non-recursive structure, so it is stable in theory or in practice, and the error is small. Because of the high requirement for phase information in EEG signal analysis and the nonlinear distortion of amplitude-frequency phase in IIR filter, IIR filter is not suitable for pre-processing.

FIR digital filter has higher order because its pole is fixed at the origin and convolution operation is more than IIR. However, FIR has a strict linear phase, and the frequency characteristics can be set arbitrarily. The phase of EEG can be guaranteed to the greatest extent by using FIR filter, and important phase information can be retained. Therefore, the FIR filter is used for low pass filtering in the process of brain EMG preprocessing.

Adaptive filter

The adaptive filter is to make a difference between the reference artifact and the observed signal with artifact components, and dynamically estimate the artifact components according to the minimum mean square error criterion, and automatically adjust the filter coefficients. Finally, the best filtering is achieved, which maximally filters out artifacts and preserves useful signals. The working principle of the adaptive filter is shown in Fig. 3.

As shown in Fig. 3, the expected signal $\varepsilon(i)$ is:

$$\varepsilon(i) = s(i) - y(i) \tag{1}$$

The output $y(i)$ of the adaptive filter is:

$$y(i) = W(i)^T - X(i) \tag{2}$$

The iterative formula of the weight coefficient of the adaptive filter is:

$$w(i+1) = w(i) + \beta\varepsilon(i)x(i) \tag{3}$$

Among them, β is the global step size.

An example is given to demonstrate the effectiveness of the adaptive filter in eliminating power-frequency interference in a segment of EEG signal with power-frequency interference, such as Fig. 4a and b. The time-domain waveform and spectrum of the 50 Hz signal after notching by adaptive filter are shown in Fig. 4c and d. It can be seen that the 50 Hz power frequency can be effectively removed.

Moving segment detection method based on EMG signal

Active segment detection is an important step in the process of motion pattern recognition based on multi-channel EMG signals. Its purpose is to extract the signal corresponding to the execution of the action in the data stream of multi-channel continuous acquisition of EMG signals.

Active segment detection is a method that can effectively judge the action mode data segment. Although the EMG preconditioning algorithm in the previous section can effectively suppress the existence of interference noise in the collected EMG data, it can not guarantee that all of them are caused by arm mode action. How to determine the start and end point of the action plays a key role in the accurate identification of arm mode. At present, the existing algorithms for extracting active segments of sEMG include Self-organizing Artificial Neural network, short-time Fourier transform and moving average.

In the design method of moving window detection active segment, firstly, the EMG signal is smoothed, and then the obtained data are compared with the set threshold one by one. When the threshold value is greater than, it is considered to be an active point, and the continuous accumulation of active points is greater than w (active points), it is considered to be the beginning of an action. If the data is less than the threshold value, it is considered as inactive point, and the number of inactive points is less than w, that is, the end of the point action. The specific steps are as follows:

Step 1: The average sEMG signal sequence$s_c(t)$, which can reflect the movement time and relaxation time of arm movement mode, is obtained by summing the sEMG signal $\bar{s}(t)$ of each channel, where $1 \le c \le C$, as shown in formula (4) below.

$$\bar{s}(t) = \frac{1}{C}\sum_{c=1}^{C} s_c(t) \tag{4}$$

Furthermore, the signal instantaneous energy sequence $E(t)$ can be obtained by square calculation of $\bar{s}(t)$, as shown in formula (5).

$$E(t) = \bar{s}(t)^2 \tag{5}$$

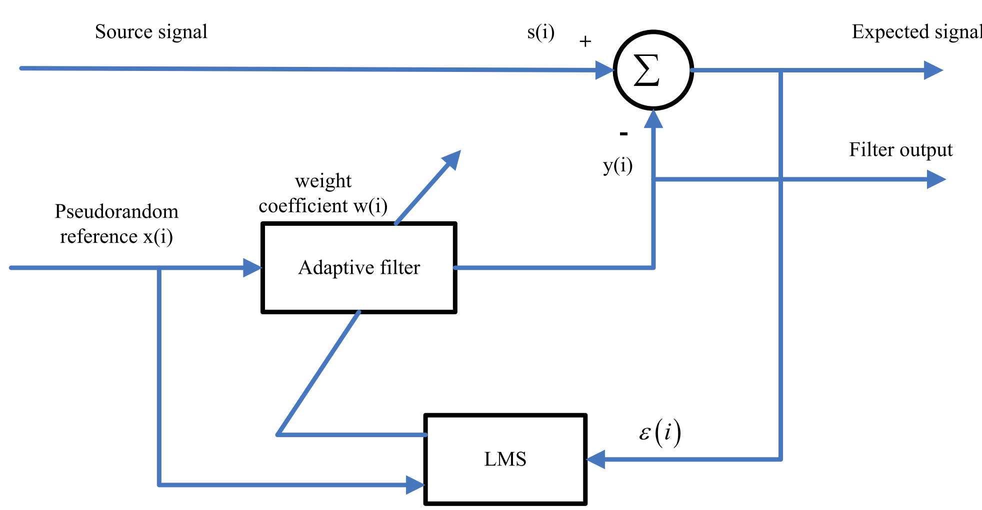

Fig. 3 Working principle of adaptive filter

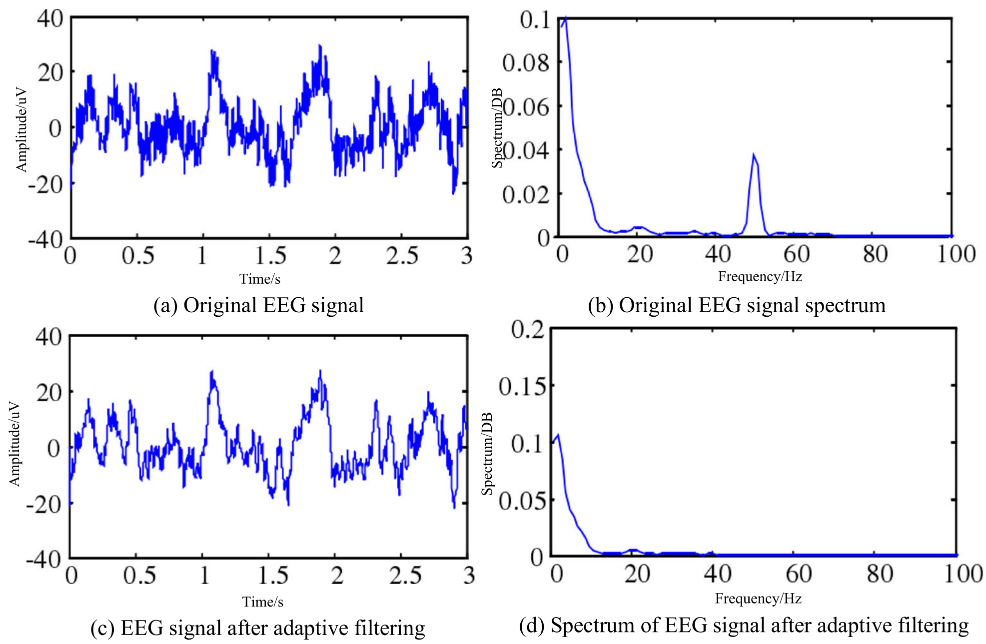

Fig. 4 Removal of power frequency interference by adaptive filter

Step 2: Selecting the width of the active window as w = 64, the instantaneous energy sequence of the above signals is processed by moving average, and the moving average sequence $E_{MA}(t)$ is obtained, as shown in formula (6), where $t > w$.

$$E_{MA}(t) = \frac{1}{w} \sum_{i=t-w+1}^{t} E(i) \tag{6}$$

Step 3: In order to determine the starting point and the ending point of the active segment, the corresponding threshold TH is selected, and the $E_{MA}(t)$ processed by the moving average is further analyzed. The starting point is that the moving average signal just exceeds TH, and 64 consecutive points all exceed TH. The end point is the point where the moving average signal is just below, and the 64 consecutive points are below TH.

Step 4: According to the starting and ending points obtained above, the active segment whose length of data points is less than a certain value (500 ms or 500 data points in this paper) is taken as noise.

In the above steps, because the threshold TH is mainly affected by the signal-to-noise ratio of EMG signal, the selection of the threshold TH is mainly based on the actual application effect. In view of the good quality of the signal obtained by the sEMG sensor in the experiment, the TH value is selected as 2% of the instantaneous peak energy of the signal.

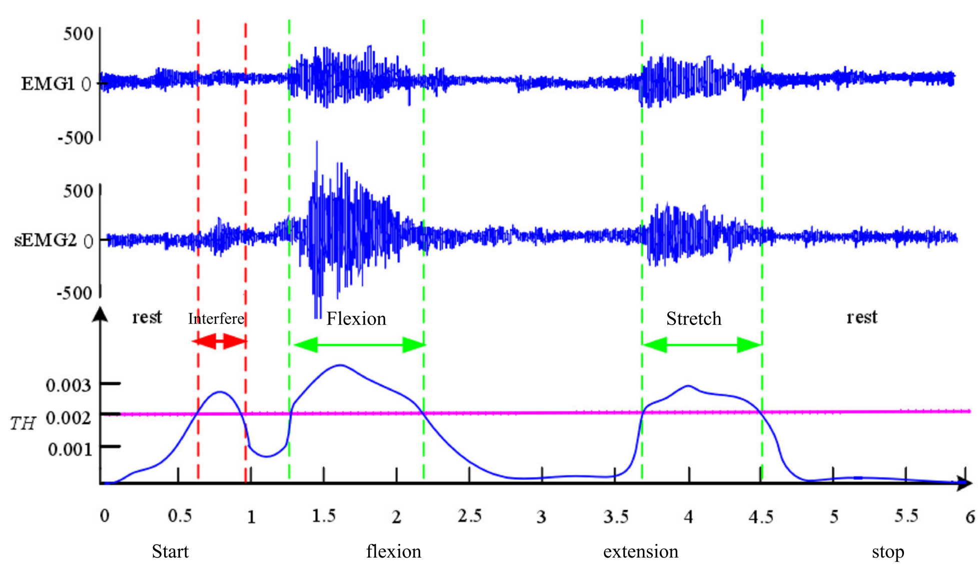

Fig. 5 EMG activity segment analysis

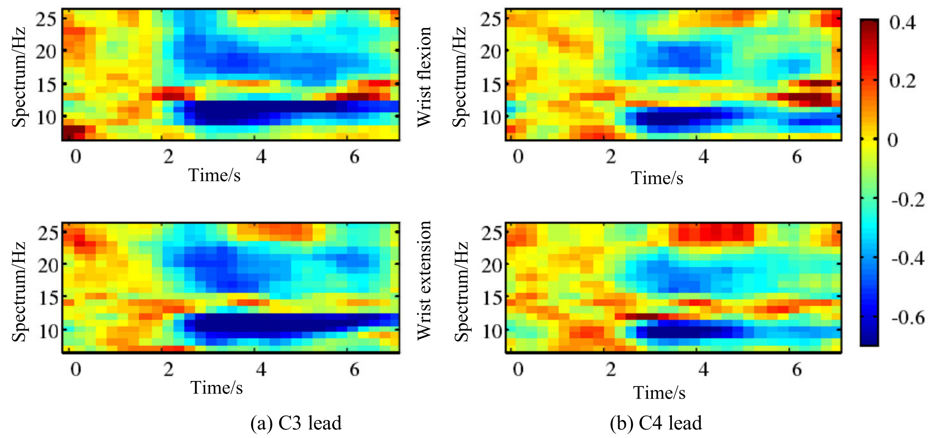

Fig. 6 ERD/ERS time-frequency analysis of S2 in wrist flexion and extension

The starting and ending points of the movement are obtained by the above moving segment detection method, and then the moving segments of the multi-channel SEMG signals corresponding to different arm movements are determined. Figure 5 shows a healthy volunteer completing the flexion and extension of the arm, obtaining sEMG1 of biceps brachii and sEMG2 of triceps brachii, and then using the moving window method to detect the active segments of flexion and extension. According to the graph, before the flexion and extension movement, there is a section of interference signal which is removed, and the starting point of the flexion movement is 1.25 s and the ending point is 2.20s. The starting point of the extension movement is 3.58 s and the ending point is 4.5 s, which is very consistent with the actual movement.

Research on fusion and synchronization analysis system of brain electromyography

Data acquisition steps

Nine healthy subjects (one female and one college student) without any medical history were selected. All the subjects signed informed consent. The experiment was conducted in a quiet shielded room with subjects sitting in comfortable seats at a horizontal distance of 80 cm from the screen. According to the screen hints, the corresponding wrist flexion and movement imagination is performed, and the wrist flexion and extension movements are performed. To avoid mental fatigue, the experiment was divided into two parts, each containing 40 trials, 20 flexions and 20 extensions. A single trial lasted for 7S, and the specific experimental process consisted of 3 steps.

Table 1 Significant frequency range of ERD per subject

Subject	Frequency band/Hz	Frequency band/Hz
S1	8,10	13,18
S2	10,12	20,24
S3	8,10	20,32
S4	8,10	20,25
S5	10,14	15,35
S6	10,12	20,25
S7	10,13	18,22
S8	10,14	12,24
S9	8,10	16,28

Step 1: When $t = 0$–2 s, a "ten" cursor appeared in the center of the screen, accompanied by a brief buzz to remind the subject that the experiment was about to begin, and that attention should be focused on waiting for the action prompt instructions to appear.

Step 2: The pictures of wrist extension / flexion movement appeared on the screen of $T = 2$–5 s. The subjects imagined the wrist extension / flexion movement and did the corresponding movements according to the pictures. The order of the two movements was random.

Step 3: At $t = 5$–7 s, the monitor was in black screen and the subjects were resting at 2S.

Neuroscan EEG acquisition system was used to collect EEG and EMG signals synchronously. Select the mastoid part as the electrode reference, AFZ forehead central grounding, while acquiring horizontal and vertical two channels of electroocular signals. The reserved channel of Neuroscan EEG acquisition system was used to collect the EMG signals of ulnar flexor carpi and extensor carpi longus. The sampling frequency is set to 1000 Hz and 50 Hz notch processing is adopted.

Since the ERD / ERS characteristics of EEG signals are mainly embodied in alpha band (8–12 Hz) and beta band (13–30 Hz), the original EEG signals are filtered by 5–40 Hz band-pass filter, and the noise interference caused by baseline drift is eliminated. Independent component analysis (ICA) is used to remove the artifacts of electromyography (EMG), and the EMG signal is preprocessed. The power frequency interference is removed by

Table 2 Subject α band ERD quantified value

Subject	Wrist bending				Wrist extension			
	C3		C4		C3		C4	
	0–2 s ERD	3–5 s ERD	0–2 s ERD	3–5 s ERD	0–2 s ERD	3–5 s ERD	0–2 s ERD	3–5 s ERD
Mean	0.06933	−0.41544	0.09689	−0.33755	0.09498	−0.42756	0.08898	−0.35333
Variance	0.076981	0.037229	0.022627	0.027512	0.023524	0.038762	0.02779	0.051189
Significant	<0.01		<0.01		<0.01		<0.01	

adaptive filter, and then the effective band of EMG signal is extracted by 10–200 Hz band-pass filter.

EEG characteristics analysis

The ERD / ERS produced in the motor process mainly appeared in the sensorimotor area of the cerebral cortex. The EEG signals of C3 and C4 channels were analyzed. The average ERD / ERS of all trials were calculated and smoothed with window. Figure 6 shows the ERD / ERS of C3 and C4 leads under flexion and extension of S2 right wrist. As can be seen from the graph: (1) from the time domain performance of ERD/ERS, S2 is basically the same as S1. (2) According to the frequency distribution of ERD/ERS, the ERD phenomena mainly occur in the high α frequency band (10–12 Hz) and the low β frequency band (15–20 Hz). (3) There was no significant difference in ERD between wrist flexion and extension.

The same analysis was performed on the other seven subjects. Table 1 shows the significant bands of ERD in each subject. It can be seen that the significant bands of ERD in all subjects are concentrated in the α band (8–12 Hz) and β band (1330 Hz). To further quantify the ERD phenomena in wrist bending and stretching, Table 2 gives the results of the baseline reference time (0–2 s), the ERD quantified mean value in the action time (3–5 s) and the paired sample t-test of ERD in all subjects.

Analysis of EMG characteristics

The electromyogram (EMG) signals of the ulnar flexor carpi (FCU) and radial extensor carpi longus (ECRL) were preprocessed and the integral EMG values were calculated every 1000 points (1 s). When wrist flexion (2–5 s), the amplitude and integral EMG of FCU were significantly higher than ECRL, and when the action returned (5–7 s), the amplitude and integral EMG of FCU decreased, while the amplitude and integral EMG of ECRL increased slightly, indicating that ECRL participated in the execution of the return action. When the wrist was stretched, the EMG amplitude and integral EMG of ECRL were significantly higher than that of FCU. When the action returned, the EMG amplitude and integral EMG of ECRL and FCU decreased to near zero.

For healthy people, wrist bending and stretching can be effectively identified by solely integrating electromyographic features. However, the EMG signals of patients with motor dysfunction are extremely weak, and fatigue and muscle weakness may occur during long-term exercise. Figure 7 EMG signals of biceps brachii on the affected side and the contralateral side was collected from a stroke patient (paralysis of right upper limb due to cerebral hemorrhage) under arm flexion and extension mode. The amplitude of EMG signals on the affected side was significantly lower than that on the contralateral side. Studies have shown that with the increase of fatigue, the motor nervous system will recruit more peripheral motor neurons to maintain a constant output of force, resulting in an increase in EMG amplitude, but then when the force can not be maintained constant, the EMG amplitude will drop sharply. Therefore, by fusing with EEG signals, the accuracy of motion recognition can be improved by making use of their synergy and complementarity. Due to the limitation of experimental conditions, the EMG signal amplitude of healthy subjects was degraded to simulate the EMG signal of patients with different degrees of motor dysfunction or exercise

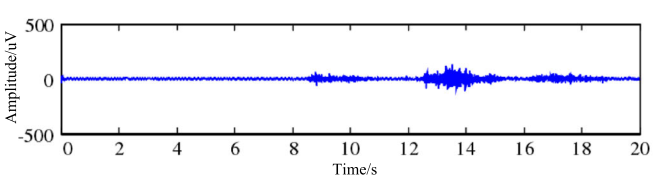

(a) EMG signal on affected side

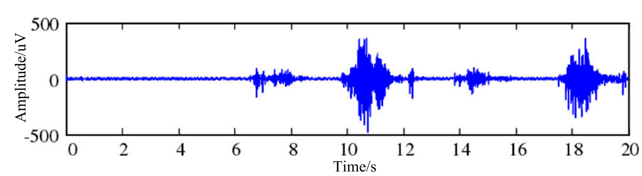

(b) Healthy sEMG signal

Fig. 7 EMG signal of patients

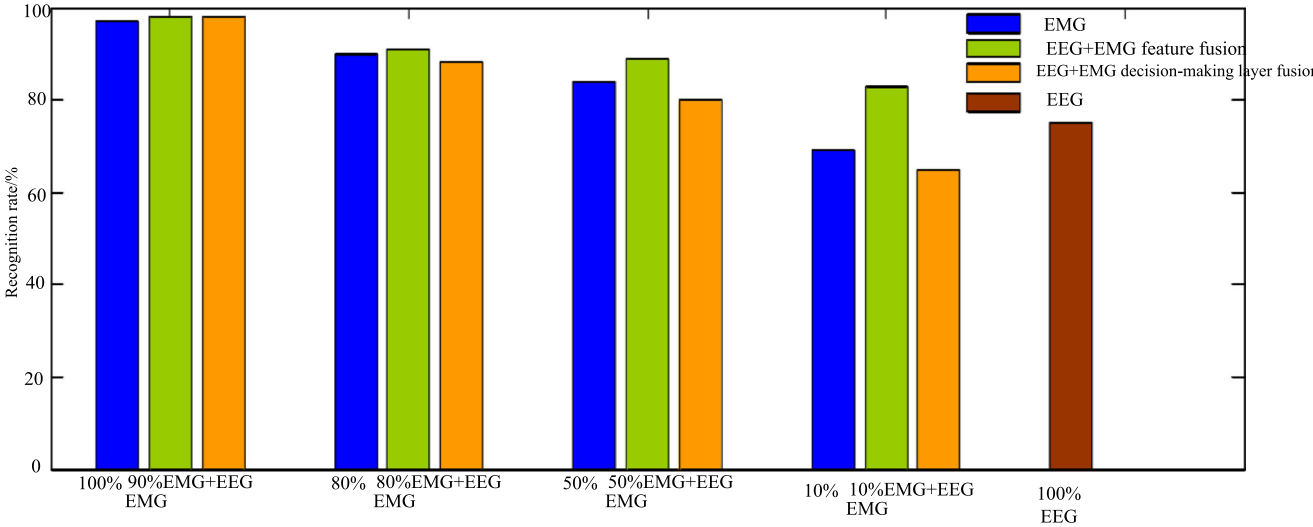

Fig. 8 Recognition accuracy is based on electromyography, EEG fusion and EEG characteristics

fatigue. The amplitude attenuation ranged from 20% to 100%, that is, 80% EMG, 50% EMG and 10% EMG, respectively.

Experimental results and analysis

After pretreatment, 794 tests (flexion: 344; extension: 350) were performed to remove the artifacts that still existed. To verify the validity of this method in BCI, six different data models were established by decreasing EMG amplitudes of all trials: EMG, 100% EMG + EEG, 80% EMG + EEG, 50% EMG + EEG, 10% EMG + EEG, EEG. After each feature is extracted, 794 sets of feature samples are obtained. For each data model, half of the feature set is randomly selected as the training set. SVM-PSO method [13] is used to search for the optimal feature fusion coefficient A and train the SVM recognition network. The other half of the feature set of all data models is classified as test set, and the trained fusion coefficients and SVM recognition network are selected by detecting the magnitude of the EMG signals in the active segment. At the same time, EEG and EMG feature vectors are sent to SVM network for training and recognition, and Bayesian network [14] is used to fuse the recognition results based on EEG and EMG separately at the decision level.

Table 3 Variation results of fusion coefficients under different myoelectric amplitudes

Characteristic source	Fusion coefficient			
	EEG		EMG	
	a_1	a_2	a_3	a_4
80%EMG + EEG	0.65	0.32	1.39	1.98
50%EMG + EEG	0.92	0.67	1.16	1.51
10%EMG + EEG	1.93	0.98	0.77	0.76

Figure 8 is a recognition result based on EEG or EMG alone, SVM-PSO feature fusion and Bayesian network decision level fusion. It can be seen that when EMG signal is strong, the recognition accuracy of the three recognition methods are very high. With the decrease of EMG amplitude, the accuracy of EMG feature recognition and decision-making level fusion decreased significantly. Especially when EMG signal was reduced to 10%, the result of decision-making level fusion was reduced to 65%. This is because Bayesian decision level fusion is dependent on each source recognition result, and 10% of EMG has lost the independent decision-making ability. By combining with EEG feature fusion, a more accurate and stable recognition result is achieved.

Table 3 is the corresponding change of the fusion coefficient with the decrease of the amplitude of EMG. It can be seen that in the exercise fatigue state (EMG amplitude decreased), the fusion coefficient of EMG features decreased significantly, while the fusion coefficient of EEG increased significantly, indicating that the weight of EMG features in decision-making decreased, and EEG signals played a major role in SVM network recognition process. It proves that the SVM-PSO network constructed in this paper effectively utilizes the synergistic complementarity between EMG to improve the recognition rate of the system, and by adjusting the EMG fusion coefficient to avoid the decrease of the recognition rate caused by the reduction of the amplitude of EMG signal, improves the accuracy and robustness of the motion pattern recognition and control system.

Conclusion

Aiming at the EEG data fusion rehabilitation system based on Virtual Prototyping technology, this paper uses the coordination and complementarity between EEG signal and EMG signal to study the motion pattern recognition method based on the feature fusion of EEG signal and EMG signal, so as to improve the accuracy and flexibility of the rehabilitation training system. A virtual rehabilitation training system based on EMG feedback is built, and the EMG signal feature analysis method is applied to the system to realize effective control and adaptive feedback adjustment of rehabilitation training scene. The validity of the virtual rehabilitation system is validated by the contrast experiment between healthy people and patients, and the comparison between the traditional rehabilitation training method and the virtual rehabilitation training method is made to verify the advantages of the system compared with the traditional virtual rehabilitation system in anti-fatigue and avoiding secondary injury. Experimental results show that the proposed EEG feature fusion method improves the accuracy and stability of the limb unilateral movement pattern recognition system, and can be further applied to the hybrid brain-computer interface to achieve fine control of external equipment and help patients with rehabilitation training.

Funding This research is based upon work supported in part by the National Natural Science Foundation of China (No. 61502350).

Compliance with Ethical Standards

Ethical Approval This article does not contain any studies with human participants performed by any of the authors.

References

1. Ling, L., Xiang, C., Lu, Z. et al., Development of an EMG-ACC-based upper limb rehabilitation training system[J]. *IEEE Trans. Neural. Syst. Rehabil. Eng.* 25(3):244–253, 2016.
2. Al-Quraishi, M. S., Ishak, A. J., Ahmad, S. A. et al., Classification of ankle joint movements based on surface electromyography signals for rehabilitation robot applications[J]. *Med. Biol. Eng. Comput.* 55(5):1–12, 2017.
3. Hu, X. L., Tong, R. K., Ho, N. S. et al., Wrist rehabilitation assisted by an electromyography-driven neuromuscular electrical stimulation robot after stroke[J]. *Neurorehabil. Neural Repair* 29:767–776, 2015.
4. Miyaoka, S., and Miyaoka, Y., An electromyography-based system for measuring the flavor detection time in healthy adults[J]. *J. Behav. Brain Sci.* 3(8):581–583, 2013.
5. Yu, C., Wang, Z., Yu, Z. et al., Design of rehabilitation training system with electromyography feedback for stroke patients[J]. *Chinese Journal of Medical Instrumentation* 39(3):187–189, 2015 205.
6. Yang, G., Deng, J., Pang, G., et al. An Iot-enabled stroke rehabilitation system based on smart wearable armband and machine learning[J]. *IEEE J. Transl. Eng. Health Med.* PP(99):1–1, 2018.
7. Roset, S. A., Gonzalez, H. F., Sanchez, J. C. Development of an EEG based reinforcement learning Brain-Computer Interface system for rehabilitation.[J]. 2013:1563–1566, 2013.
8. Li, C., Rusák, Z., Horváth, I. et al., Influence of complementing a robotic upper limb rehabilitation system with video games on the engagement of the participants: A study focusing on muscle activities[J]. *Int. J. Rehabil. Res.* 37(4):334–342, 2014.
9. Liu, Y. H., Huang, H. P., Huang, T. H. et al., Controlling a rehabilitation robot with brain-machine Interface: An approach based on independent component analysis and multiple kernel learning[J]. *International Journal of Automation & Smart Technology* 3(1): 67–75, 2013.
10. Wu, S., A traffic motion object extraction algorithm[J]. *International Journal of Bifurcation and Chaos* 25(14): 1540039, 2015.
11. Wu, S., Wang, M., and Zou, Y., Research on internet information mining based on agent algorithm[J]. *Futur. Gener. Comput. Syst.* 86:598–602, 2018.
12. Wang, Q., Chen, X., Chen, R. et al., Electromyography-based locomotion pattern recognition and personal positioning toward improved context-awareness applications[J]. *IEEE Trans. Syst. Man Cybern. B* 43(5):1216–1227, 2013.
13. Yu, W., and Li, S., Recommender systems based on multiple social networks correlation[J]. *Futur. Gener. Comput. Syst.* 87: 312–327, 2018.
14. Yu, W., Li, S., Tang, X. et al., An efficient top-k ranking method for service selection based on ε-ADMOPSO algorithm[J]. *Neural Comput. & Applic.*:1–16, 2018.